

Synthesis of Cu_2O , CuCl , and Cu_2OCl_2 nanoparticles by ultrafast laser ablation of copper in liquid media

SYED HAMAD¹, G KRISHNA PODAGATLAPALLI², SURYA P TEWARI^{1,2}
and S VENUGOPAL RAO^{2,*}

¹School of Physics, University of Hyderabad, Hyderabad 500 046, India

²Advanced Centre of Research in High Energy Materials (ACRHEM), University of Hyderabad, Hyderabad 500 046, India

*Corresponding author. E-mail: svrsp@uohyd.ernet.in

DOI: 10.1007/s12043-014-0686-9; ePublication: 13 February 2014

Abstract. Copper complex nanoparticles were fabricated from bulk copper using picosecond laser ablation in water and chloroform. We found that composition of the nanoparticles was CuCl and Cu_2OCl_2 in chloroform at three different input fluences; Cu_2O in water which was confirmed from the data of EDAX, UV-Visible absorption spectra, and selected area electron diffraction pattern. We have also performed nonlinear optical studies of colloidal nanoparticles using Z-scan technique at 800 nm and ~ 2 ps laser pulses. Cu_2O NPs exhibited two-photon absorption at lower peak intensities while three-photon absorption was observed at higher peak intensities. Other samples exhibited two-photon absorption at all peak intensities.

Keywords. Picosecond; laser ablation; copper complex; nanoparticles; Z-scan.

PACS Nos 52.38.±r; 81.07.±b; 42.65.±k

1. Introduction

Investigations on metal oxide and metal halide nanoparticles have dominated recent research due to their unique properties, which are different from the pure metal nanoparticles. Copper nanoparticles (Cu NPs) are promising materials since bulk copper exhibits high thermal and electrical properties. This leads to significant applications in cooling fluids in electronic systems [1]. Due to their surface plasmons, Cu NPs exhibit enhanced nonlinear optical (NLO) properties which can lead to promising optical limiting and optical switching devices [2]. Copper oxide (Cu_2O or CuO) and copper chloride (CuCl) are semiconductors exhibiting narrow band gap and have been commonly used as catalysts [3,4]. The optical and electronic properties of semiconductor NPs are purely dependent on size. When the dimension of any material reaches nanodimensions, the energy spectrum turns discrete resulting in increase of the band gap. Recent reports suggest that Cu

and Cu₂O (or) CuO nanoparticles hold significant promise as antibacterial agents as well as NLO materials [5–7]. Laser ablation of metals in liquid media (LAL) [8] is a fast and effortless method to manipulate bulk to nanoscale materials since it does not require multistep chemical synthetic procedures, long reaction times and temperature treatments. Furthermore, LAL guarantees extremely stable NPs without the use of capping agents combined with the highest degree of occupation and safety since fabricated NPs will be in colloidal form. Moreover, ultrafast laser ablation [8] is a unique material processing technique that provides distinct advantages in applications over the nanosecond (ns) laser ablation since the near threshold ablation of metals with femtosecond (fs) and picosecond (ps) pulses exhibit a material-independent behaviour. Ultrashort laser pulses even allow less thermal damage and a nearly melt-free ablation if it is performed close to the ablation threshold. Herein we report the fabrication of Cu₂O, CuCl, and Cu₂OCl₂ NPs from the bulk Cu in water and chloroform (with different fluences) using ps ablation technique.

2. Experiment

This experiment was carried out by a 1 kHz chirped pulse amplified Ti:sapphire laser system (LEGEND, Coherent) delivering nearly bandwidth-limited laser pulses (~2 ps) at 800 nm. The amplifier was seeded with ~15 fs (55–60 nm FWHM) pulses from an oscillator (MICRA, Coherent, 1 W, 80 MHz, 800 nm). The average power from the amplifier was ~2 W. The laser beam was focussed on the Cu substrate immersed in the Pyrex cell with liquids (water and chloroform). The theoretical beam diameter estimated at the focal point on the substrate was ~30 μm. The typical level of liquid above the metal surface was ~5 mm. Typical pulse fluences used were ~7 J/cm², ~14 J/cm² and ~28 J/cm². The target was placed normal to the laser beam on a motorized X-Y stage which was controlled by a motion controller. The motorized stages (Newport) were translated in such a way to draw periodic lines on the substrates at a separation of ~50 μm. The colloids were prepared with two different scanning speeds of X-Y stages: (a) 0.1 mm/s in each direction for 28 J/cm² in water, 28 J/cm² and 14 J/cm² in chloroform and (b) 0.01 mm/s in each direction for 7 J/cm² in chloroform. The prepared Cu colloids are designated as CL-1, CL-2, CL-3, and CL-4, respectively, to address them without ambiguity. Time of exposure was ~30 min. Surface morphology, size distribution, metallic nature and oxidation fingerprints of nanoparticles were characterized by TEM, selected area electron diffraction pattern, EDAX and UV–Vis absorption spectroscopy. NLO properties of colloidal solutions were studied using the standard Z-scan technique.

3. Results and discussion

The shape and size distribution of colloidal nanoparticles in water (CL-1) and chloroform (CL-2) were confirmed by TEM analysis, data of which are shown in figures 1a and 1c, respectively, and insets show the size distribution of NPs. The size distribution was fitted with a Gaussian curve. It was confirmed that the shape of NPs were spherical in nature and the average size of the NP was ~21 nm in CL-1 and ~3.7 nm in CL-2. As observed from TEM images, the majority of produced nanoparticles were small in

size and larger sized NPs were also present but lesser in number. The size reduction of nanoparticles is credited to the photofragmentation effect [9]. Figure 1b illustrates the EDAX spectrum of CL-1 and the spectra reveal the Cu and oxygen peaks and it was confirmed that copper oxide NPs were formed in water. Inset of figure 1b (top portion and bottom portion) shows the UV-Vis absorption spectra and SAED pattern, respectively. UV-Vis absorption spectra of colloidal NPs in water demonstrated that the localized surface plasmon resonance peak (LSPR) occurred near 600 nm (corresponding to grey color of the sample) suggesting that the SPR peak shifted to longer wavelengths. The observed inconsistency was most likely the signature of fast formation of oxide layer around the particles. Similar SPR peaks of copper oxide nanoparticles have been reported earlier [10]. Another absorption peak observed in the UV spectral region (near 289 nm) could be due to metal interband transitions [10]. This is due to the reaction of copper metal with oxygen to form some metal products such as copper oxide and hydroxide. The SAED

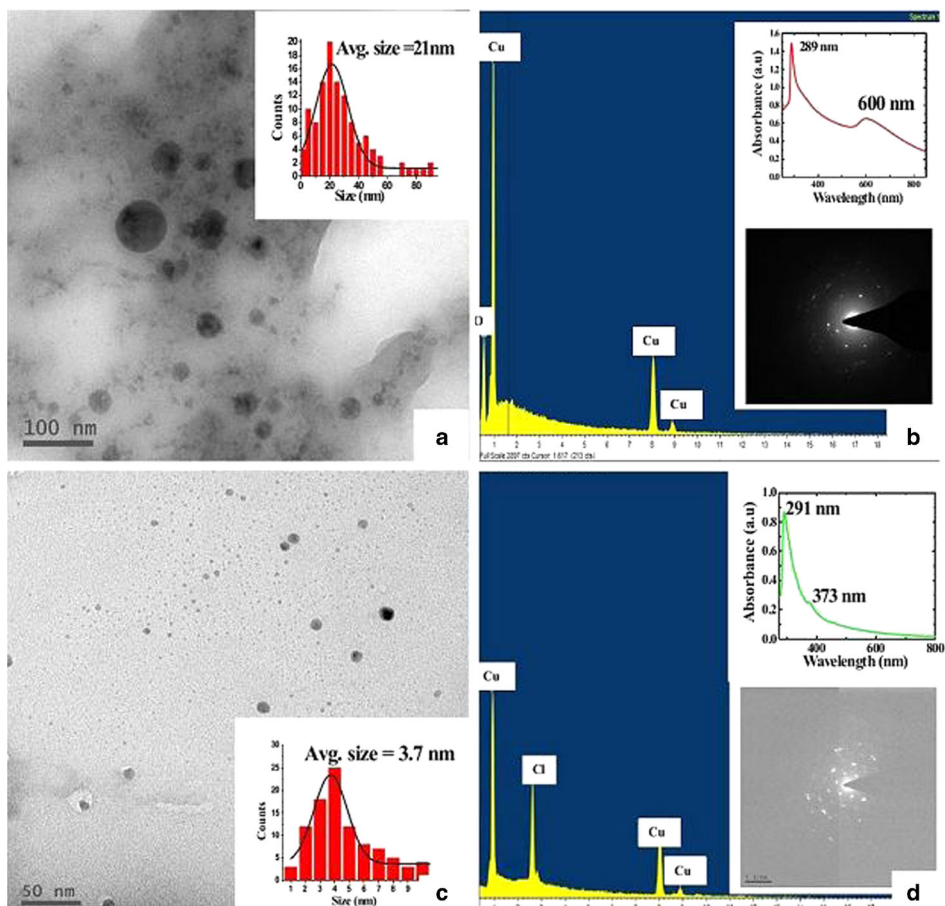


Figure 1. TEM images of (a) CL-1, (c) CL-2 and insets show the particle distribution graphs. EDAX spectra of (b) CL-1, (d) CL-2 and the insets show (above) UV-Vis absorption spectra and (below) SEAD pattern.

pattern consisted of concentric circles which confirmed the polycrystalline nature. The measured lattice interplanar spacing values (2.26 Å and 1.28 Å) agree with those of Cu₂O crystal planes. Figure 1d represents the EDAX spectrum of CL-2 and spectrum demonstrates the presence of Cu and chloride peaks. Inset of figure 1d (top part) represents the UV-Vis absorption spectra and (bottom part) SAED pattern of CL-2. The UV-Vis absorption spectrum of CL-2 depicts the characteristic absorption peak near 373 nm and another broad peak near 291 nm. Peak near 373 nm can be accredited to copper chloride NPs while the peak at 291 nm represents chlorocuprate complex [11]. SAED patterns of CL-2 confirmed the single crystalline nature and the measured interplanar spacing values (2.85 Å and 2.47 Å) agree very well with those of CuCl crystal planes.

The TEM micrographs of colloidal Cu complex NPs in chloroform for fluences of 14 J/cm² (CL-3) and 7 J/cm² (CL-4) (speed of 0.01 mm/s) are shown in figures 2a and 2c, respectively. Insets of figures 2a and 2c present the size distribution plots. As in

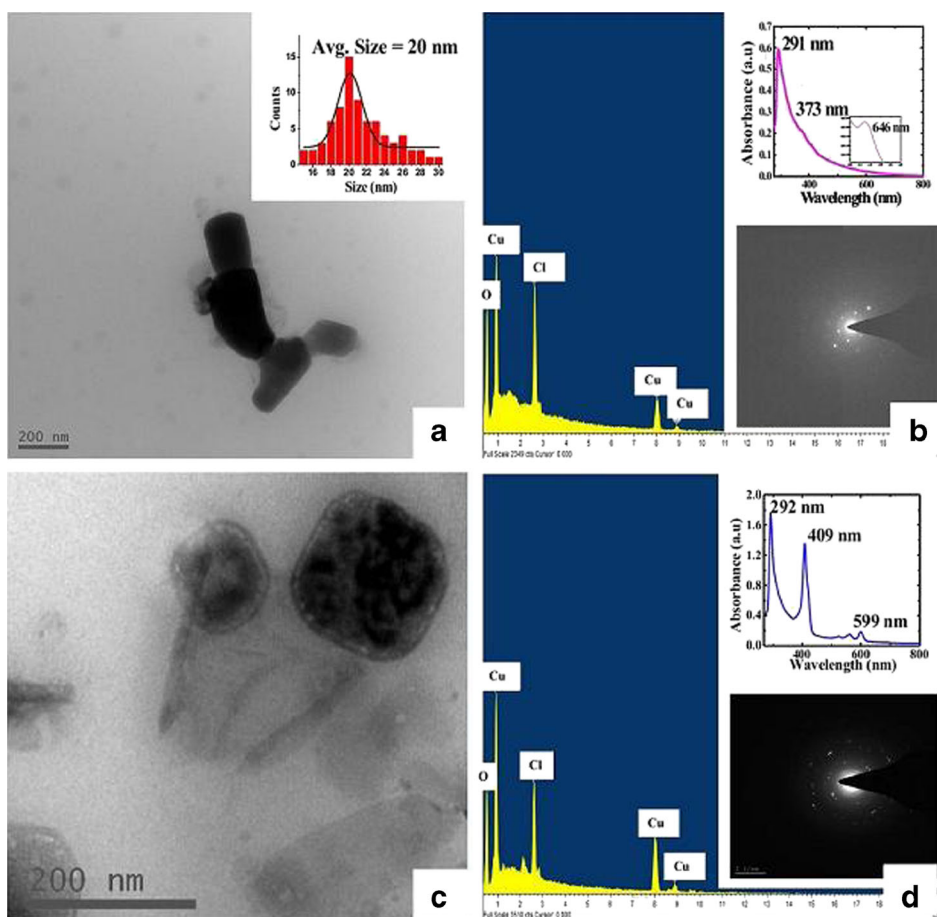


Figure 2. TEM images of (a) CL-3, (c) CL-4 and insets show the particle distribution graphs. EDAX spectra of (b) CL-3, (d) CL-4 and the insets show (above) UV-Vis absorption spectra and (below) SEAD pattern.

CL-3, we observed two shapes of NPs. One type was spherical 15–30 nm particles with an average size of ~ 20 nm. The other type of NPs was cubic. The mean size of these colloidal NPs was ~ 200 nm. For CL-4 the shape of the nanoparticles was only cubic and average size of the NPs was ~ 90 nm. As seen from the TEM image, it is evident that there is a shell around the nanocube. This might be because of oxidation of nanocube. Figures 2b and 2d represent the EDAX spectra of CL-3 and CL-4, respectively. The EDAX spectra of CL-3 and CL-4 demonstrated that Cu, chloride, and oxygen peaks were present. Insets of figures 2b and 2d represent the UV–Vis absorption spectra (top) and SAED pattern (bottom) of CL-3 and CL-4, respectively. The UV–Vis absorption spectrum of CL-3 depicted the SPR peaks near 373 nm, 646 nm and one broad peak near 291 nm. For CL-4, characteristic absorption peaks were observed near 409 nm and 599 nm, along with a broad peak near 291 nm. The peaks around 373 nm and 409 nm can be accredited to absorption in copper chloride NPs, the peak at 291 nm represents chlorocuprate complex and the peaks near 599 nm and 646 nm can be attributed to copper oxide NPs. Ganesh *et al* [11] reported that copper chloride NPs show the absorption peaks near 371 nm and 381 nm. SAED pattern of CL-3 and CL-4 consisted of three concentric rings confirming the polycrystalline nature in both cases. For CL-3, the measured interplanar spacing values (4.88 Å, 2.5 Å, and 1.4 Å) agree with those of Cu_2OCl_2 planes. In the case of CL-4, it was confirmed that crystalline lattice fringes with interplanar spacings of 5.24 Å, 3.38 Å, and 1.47 Å correspond to the crystal planes of Cu_2OCl_2 lattice. The NLO properties of Cu_2O NPs (CL-1), CuCl NPs (CL-2), and Cu_2OCl_2 NPs (CL-3 and CL-4) were studied with 1 kHz, 800 nm laser pulses

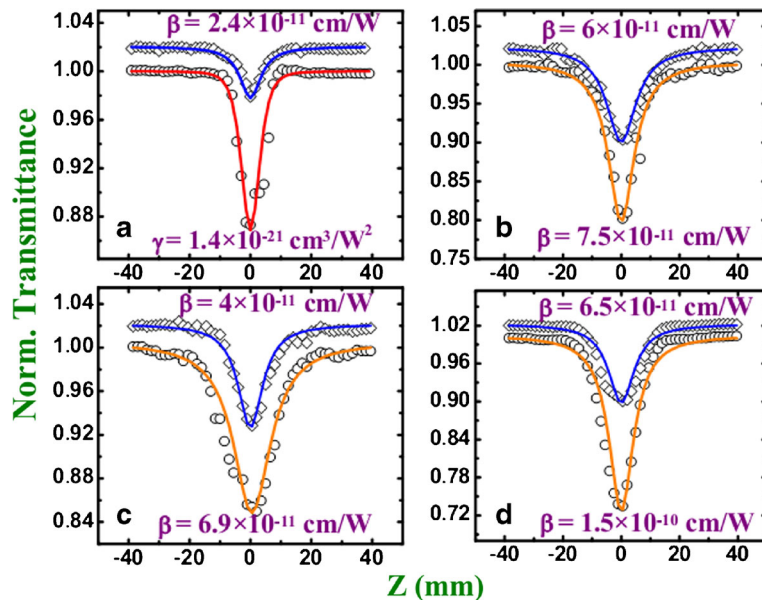


Figure 3. The open aperture Z-scan data obtained with varying input intensities 60 GW/cm^2 (open squares) and 110 GW/cm^2 (open circles) for (a) CL-1, (b) CL-2, (c) CL-3, and (d) CL-4.

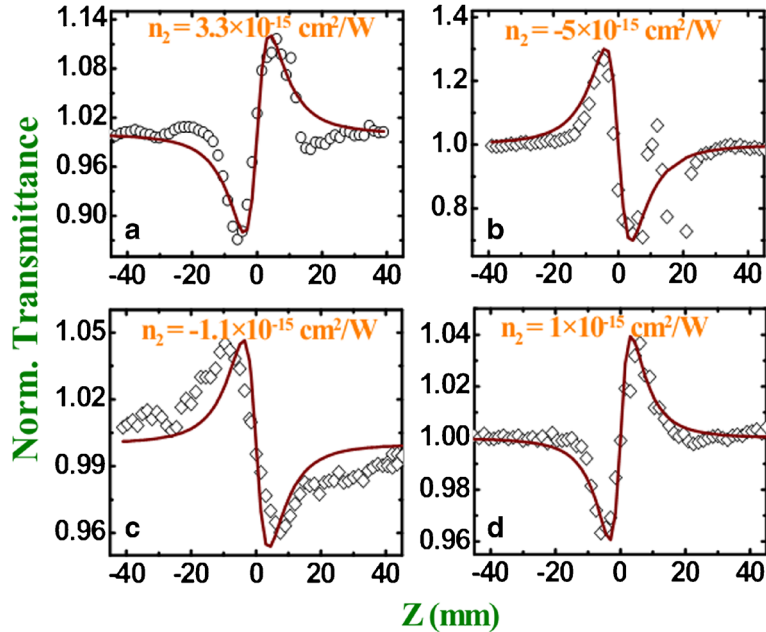


Figure 4. Closed aperture Z-scan data obtained at an input intensity of 28 GW/cm^2 (open squares) of (a) CL-1, (b) CL-2, (c) CL-3, and (d) CL-4. Solid lines are theoretical fits.

($\sim 2 \text{ mJ}$, $\sim 2 \text{ ps}$ duration). Complete details of the set-up are reported in our earlier works [12–15]. The beam waist at the focus was estimated to be $\sim 30 \mu\text{m}$. Our Z-scan data clearly demonstrated strong NLO coefficients for these colloids. Figure 3a shows open aperture data recorded for Cu_2O NPs (CL-1) in water at two different intensities clearly illustrating pure two-photon absorption (2PA) at lower peak intensity (60 GW/cm^2) and effective three-photon absorption (3PA) at higher peak intensity (110 GW/cm^2). Figures 3b and 3c illustrate the open aperture data of CuCl NPs (CL-2), Cu_2OCl_2 NPs (CL-3), and Cu_2OCl_2 (CL-4) in chloroform with strong 2PA coefficients (up to 0.1 cm/GW) obtained at both peak intensities. Figures 4a and 4d represent the closed aperture data of CL-1, CL-2, CL-3, and CL-4, respectively. The measured nonlinear refractive index was $\sim 10^{-15} \text{ cm}^2/\text{W}$ in both the cases.

4. Conclusions

To summarize, an extensive study related to fabrication of copper complex NPs via picosecond laser ablation in water and chloroform (for three different fluences) was carried out. TEM was employed for characterizing the size and shape of the particles. In both the media, the particles were spherical and it was found that the average diameters of the NPs were 21 and 3.7 nm in water and chloroform ablated at a fluence of 28 J/cm^2 , respectively while at other fluences, cubical NPs were observed. Cu_2O NPs were observed

in water, CuCl NPs and Cu₂OCl₂ NPs were observed in chloroform and was confirmed by recording the EDAX spectra, UV–Vis absorption spectra, and SAED patterns. NLO studies of colloidal Cu complex NPs were also performed and we recorded strong nonlinear optical coefficients for these NPs.

References

- [1] H S Kim, S R Dhage, D E Shim and H T Hahn, *Appl. Phys. A* **88**, 97791 (2009)
- [2] C Wu, B P Mosher and T Zeng, *Mater. Res. Soc. Symp. Proc.* **879EZ6**, 1 (2005)
- [3] M Samim, N K Kaushik and A Maitra, *Bull. Mater. Sci.* **30**, 535 (2007)
- [4] C Huang *et al*, *Langmuir* **25**, 13351 (2009)
- [5] A Nath, A Das, R Latha and A Khare, *Sci. Adv. Mater.* **4**, 106 (2012)
- [6] H Sekhar and D N Rao, *J. Nanopart. Res.* **14**, 976 (2012)
- [7] A Kim, N V Nikonorov, A I Sidorov *et al*, *Tech. Phys. Lett.* **37**, 401 (2011)
- [8] G Krishna, P S Hamad, S Sreedhar, S P Tewari and S V Rao, *Chem. Phys. Lett.* **530**, 93 (2012)
- [9] R M Tilaki, A Irajizad and S M Mahdavi, *Appl. Phys. A* **88**, 415 (2007)
- [10] R K Swarnkar, S C Singh and R Gopal, *Bull. Mater. Sci.* **34**, 1363 (2011)
- [11] G Suyal, M Mennig and H Schmidt, *J. Mater. Chem.* **13**, 1783 (2003)
- [12] S Hamad, L Giribabu, S P Tewari and S V Rao, *J. Porphy. Phth.* **16**, 140 (2012)
- [13] P T Anusha, D Swain, S Hamad, L Giribabu, T S Prashant, S P Tewari and S V Rao, *J. Phys. Chem. C* **116**, 17828 (2012)
- [14] D Swain, P T Anusha, T S Prashant, S P Tewari, T Sarma, P K Panda and S V Rao, *Appl. Phys. Lett.* **100**, 141109 (2012)
- [15] S V Rao, T S Prashant, T Sarma, P K Panda, D Swain and S P Tewari, *Chem. Phys. Lett.* **514**, 98 (2011)